

Improved spiral chemical shift imaging at 3 Tesla using a 32-channel integrated RF-shim coil array

Eren C. Kizildag¹, Jason P. Stockmann², Borjan Gagoski^{2,3,4}, Eva-Maria Ratai², Bastien Guerin^{2,4}, P. Ellen Grant^{2,3,4}, Lawrence L. Wald^{2,4}, Elfar Adalsteinsson^{1,2}

¹ Department of Electrical Engineering and Computer Science, Massachusetts Institute of Technology, Cambridge, MA, USA

²A. A. Martinos Center for Biomedical Imaging, Massachusetts General Hospital, Charlestown, MA, USA

³Boston Children's Hospital, Boston, MA, USA

⁴Harvard Medical School, Boston, MA, USA

Declaration of Financial Interests or Relationships

Speaker Name: **Eren Kizildag**

I have no financial interests or relationships to disclose with regard to the subject matter of this presentation.

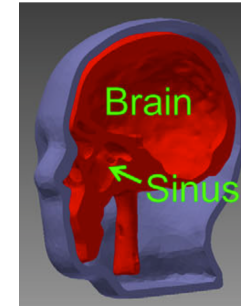
□ Motivation :

- ❖ Chemical shift imaging and shimming
- ❖ Multi-coil shim array

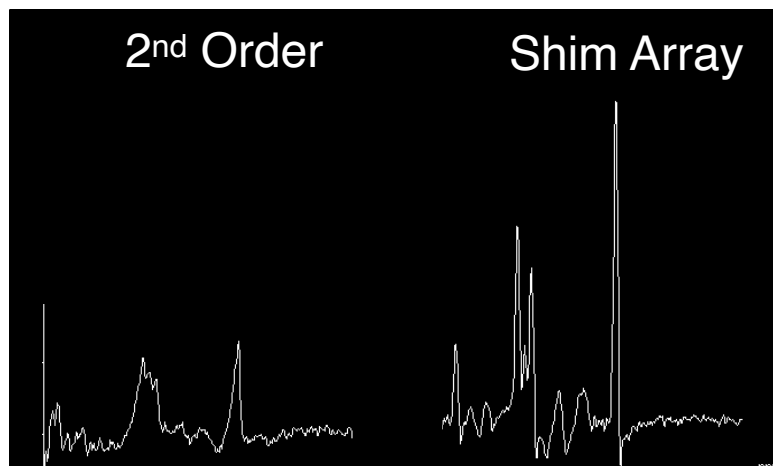


□ Experimental methods

- ❖ Phantom
- ❖ Shimming
- ❖ Acquisition



□ Results



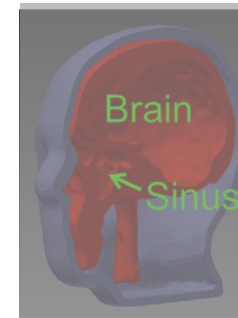
□ Motivation :

- ❖ Chemical shift imaging and shimming
- ❖ Multi-coil shim array



□ Experimental methods

- ❖ Phantom
- ❖ Shimming
- ❖ Acquisition

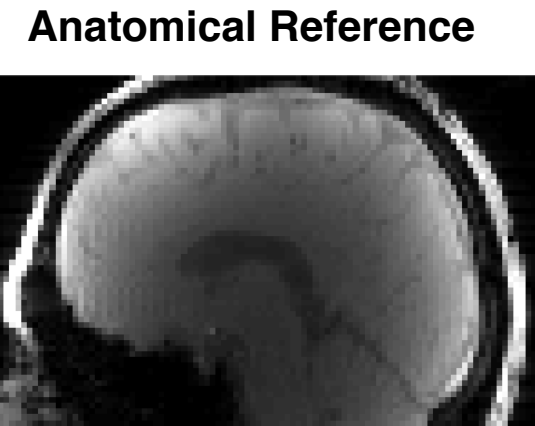
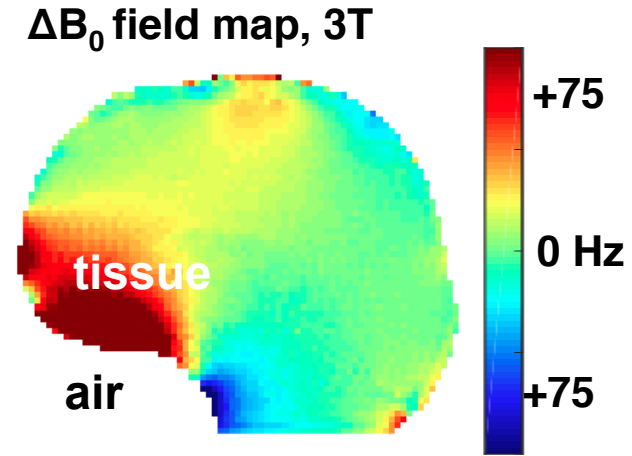


□ Results

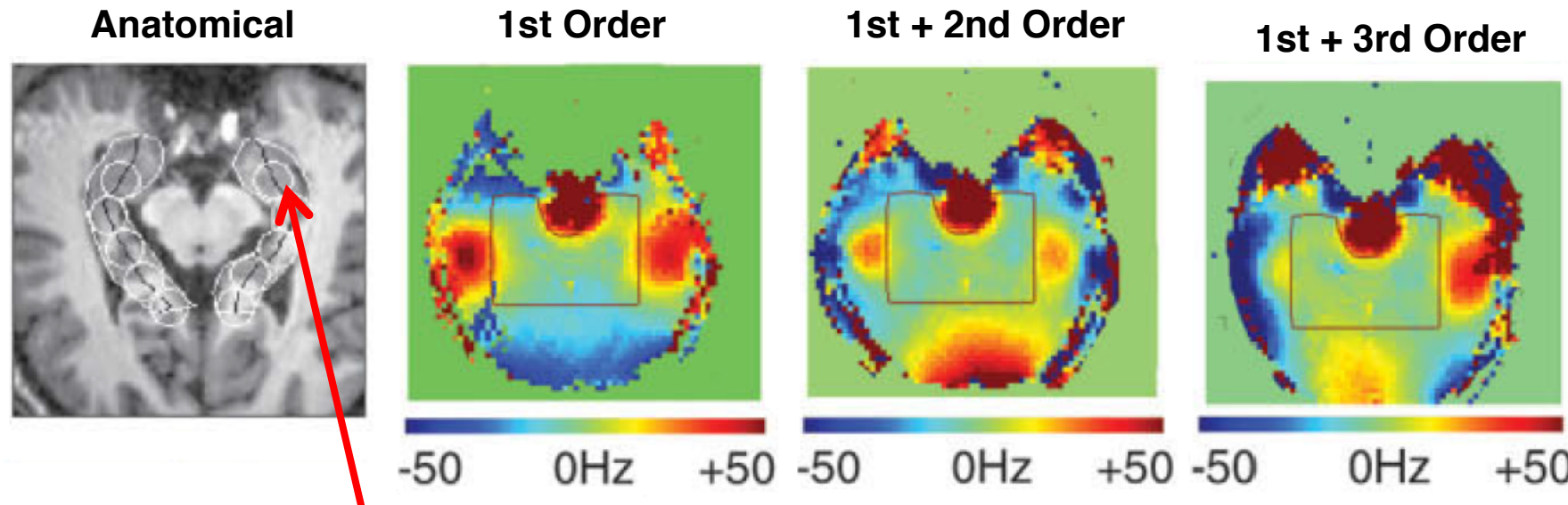


Motivation : Chemical Shift Imaging

- ❑ *In vivo* chemical shift imaging (CSI)
 - ❖ Enables to study brain metabolites
- ❑ Good B_0 shimming is critical
 - ❖ Linewidth
 - ❖ Chemical shift
 - ❖ Water and lipid suppression



Motivation : Shimming in Chemical Shift Imaging



Spectra from most anterior location:



Hetherington et al., MRM (2006)

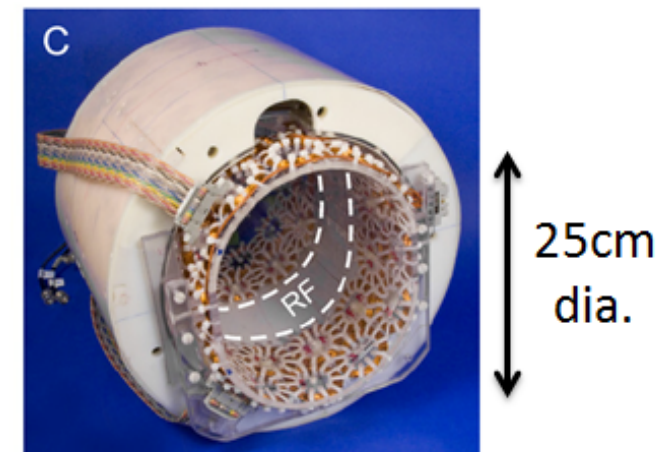
Motivation : Multi-coil (MC) Shim Array

- ❑ Drawbacks of higher-order spherical harmonics
- *Pan JW, MRM 68:1007–1017 (2012)*
 - ❖ *High inductance*
 - ❖ *Eddy currents in cryostat; need pre-emphasis for dynamic shimming*
 - ❖ *Lower efficiency at higher orders*
 - ❖ *Expensive shim current drivers*



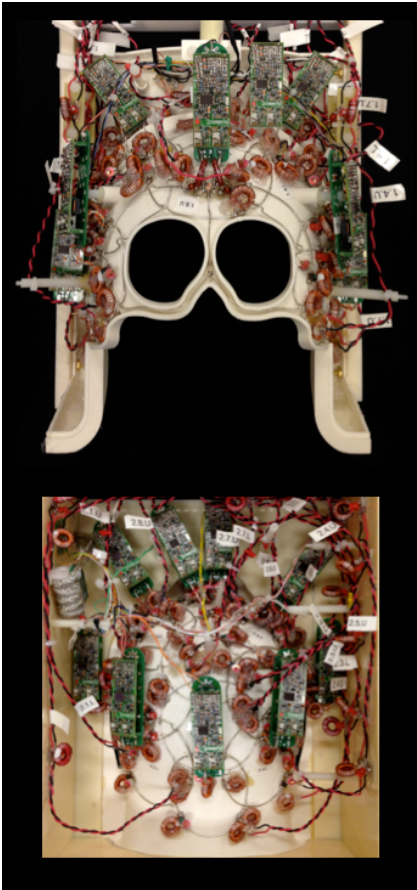
Source: Resonance Research, Inc.
<http://www.rricorp.com>

- ❑ Multi-coil shim arrays
- *Juchem C, JMR 212:280–288 (2011)*
 - ❖ *Low inductance*
 - ❖ *More efficient at generating higher-order fields*
 - ❖ *Low-cost shim current supplies*
 - ❖ *Little coupling to cryostat or gradient coils; no need for pre-emphasis*



Source: Juchem C, JMR 2011

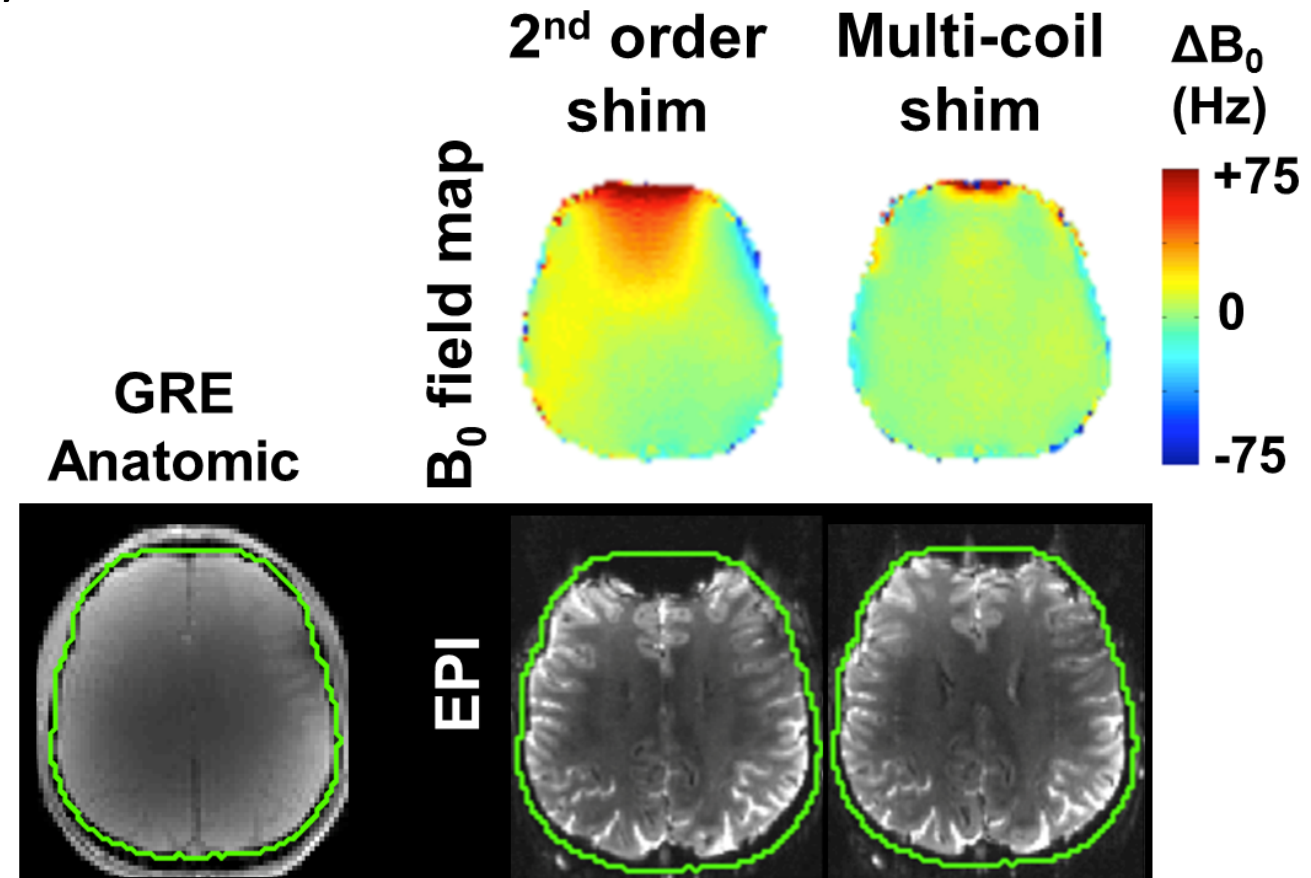
Integrated Multi-coil (MC) Shim Array



A 32-channel integrated RF-shim coil uses the same close-fitting array of loops for RF signal detection and B_0 shimming

Stockmann et al., MRM (2014)

- 32-channel, integrated RF-shim coil array
- Performances of both systems maintained



Reduced geometric distortion in EPI scans (1mm in-plane, 1.11ms echo spacing, GRAPPA R=1)

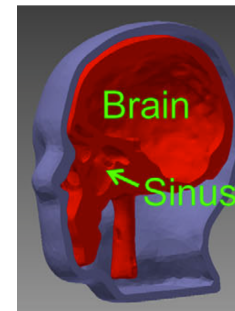
□ Motivation :

- ❖ Chemical shift imaging and shimming
- ❖ Multi-coil shim array



□ Experimental details

- ❖ Phantom
- ❖ Shimming
- ❖ Acquisition



□ Results



Experimental Details : Phantom

□ Realistic head phantom

→ Guerin et al., MRM 2015

- ❖ Brain compartment filled with 'Braino' solution

➢ NAA

➢ Cr

➢ Cho

➢ Glutamate

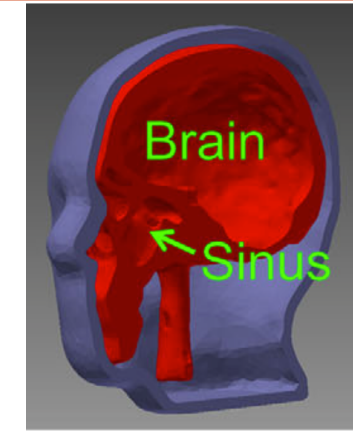
➢ GABA

➢ Myo-inositol

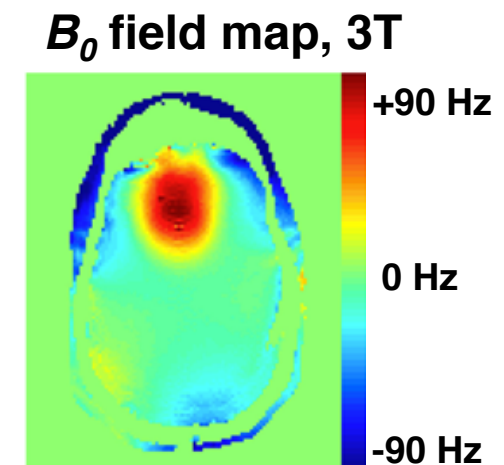
- ❖ 5x typical *in vivo* concentration

- ❖ Realistic ΔB_0 patterns observed in frontal lobes *in vivo*

- ❖ 3D models available at phantoms.martinos.org



Phantom : 3D-printed, anthropomorphic head phantom



B_0 field map, 3T

GRE experiment : axial B_0 field map, indicates indeed realistic frontal lobe B_0 profile

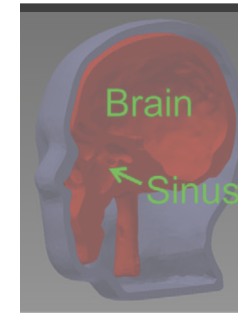
□ Motivation :

- ❖ Chemical shift imaging and shimming
- ❖ Multi-coil shim array



□ Experimental details

- ❖ Phantom
- ❖ Shimming
- ❖ Acquisition



□ Results



Experimental Details : Shimming

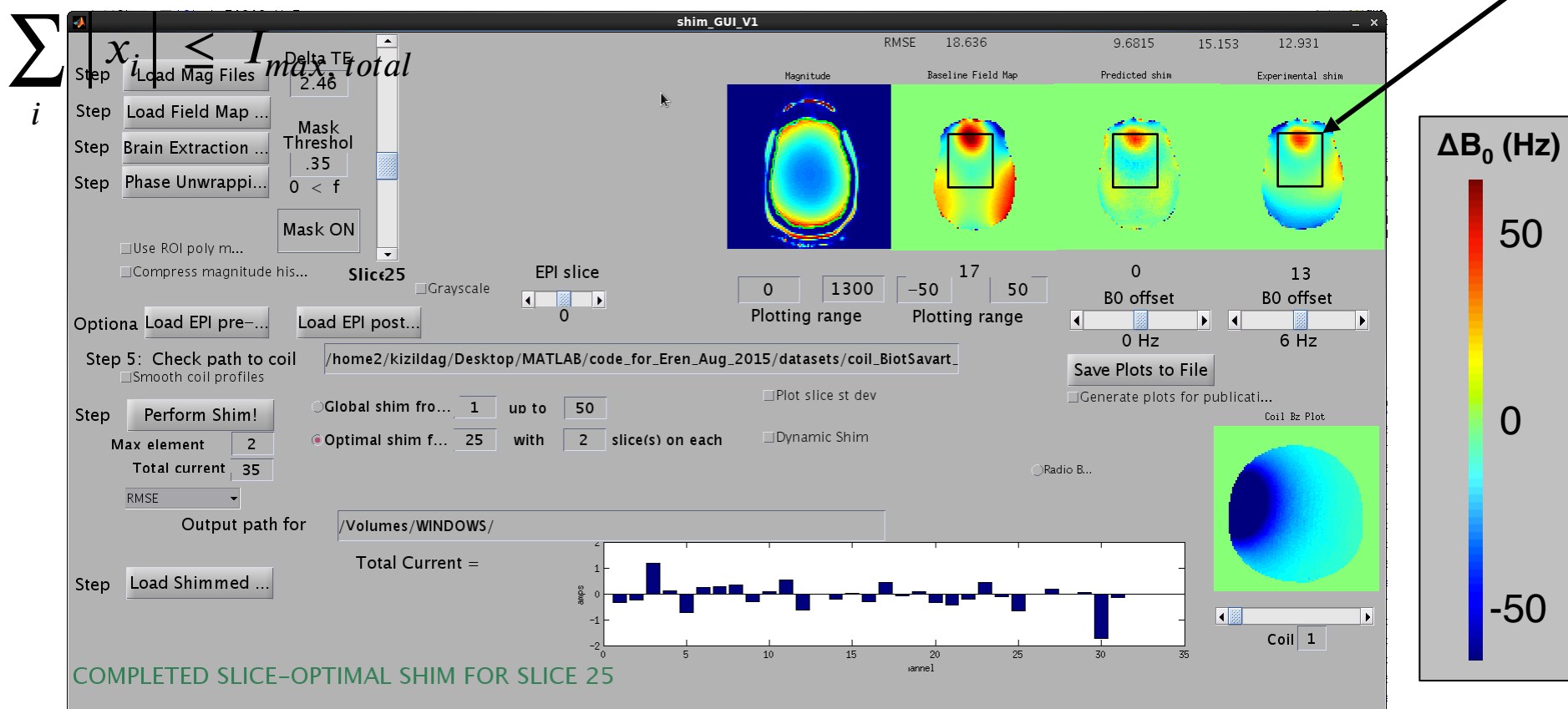
- Optimal currents computed by solving

$$\min_x \|B_0 - Ax\|_2^2$$

$$s.t \quad |x_i| \leq I_{max,loop}$$

B_0 : Baseline profile
 A : Basis set, corresponding to 1A/coil
 $I_{max,loop}$: Maximum current per loop (2.5A)
 $I_{max,total}$: Total current in the array (35A)
 x : Unknown currents to be solved

Excitation volume



Outline

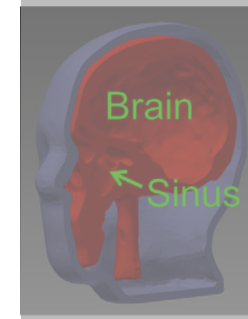
□ Motivation :

- ❖ Chemical shift imaging and shimming
- ❖ Multi-coil shim array



□ Experimental details

- ❖ Phantom
- ❖ Shimming
- ❖ Acquisition
 - ✓ Conventional Cartesian CSI



□ Results

- ❖ Conventional Cartesian CSI



Acquisition – Cartesian CSI

□ Details (CSI Acquisition)

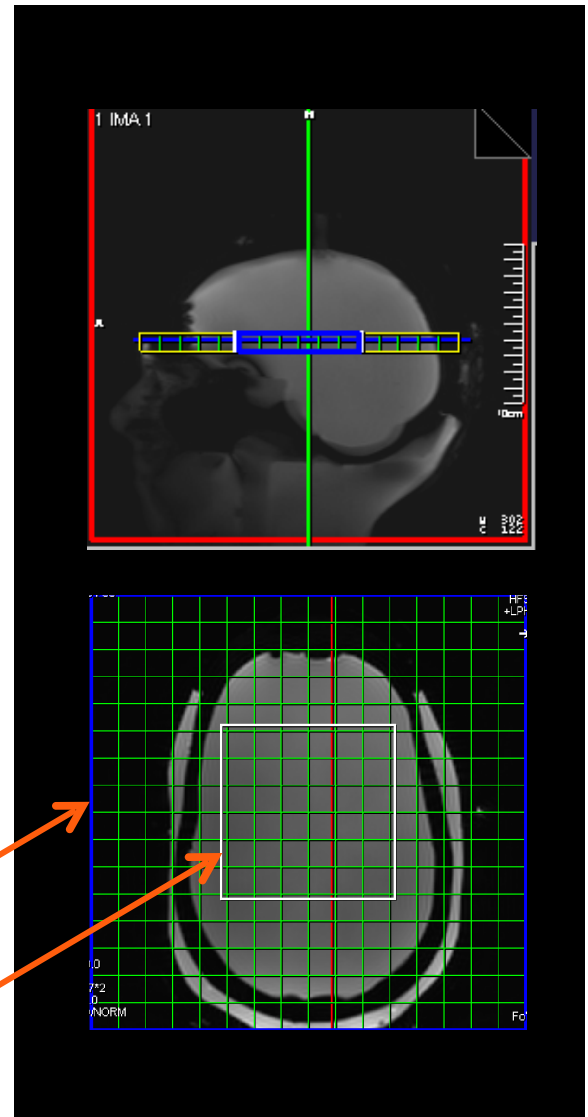
- ❖ TR/TE : 1400ms/144ms
- ❖ TA : 03:30
- ❖ Voxel : [12.5x12.5x12]mm (2cc)
- ❖ VOI : [80x80]mm

□ Acquisition Parameters (GRE):

- ❖ Resolution:
 - In-plane : 2.4mm ([240x240]mm over 100x100 matrix size)
 - Slice : 2mm
- ❖ Duration : ~2 minutes

Spatially encoded volume

LASER-excited volume



Outline

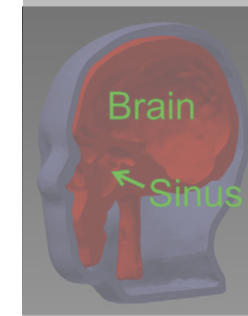
□ Motivation :

- ❖ Chemical shift imaging and shimming
- ❖ Multi-coil shim array



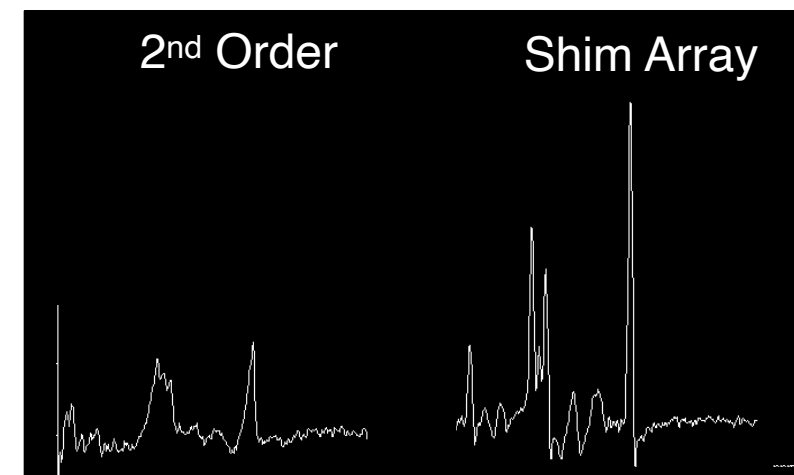
□ Experimental details

- ❖ Phantom
- ❖ Shimming
- ❖ Acquisition
- ✓ Conventional Cartesian CSI



□ Results

- ❖ Conventional Cartesian CSI



Methodology – Performance Metrics

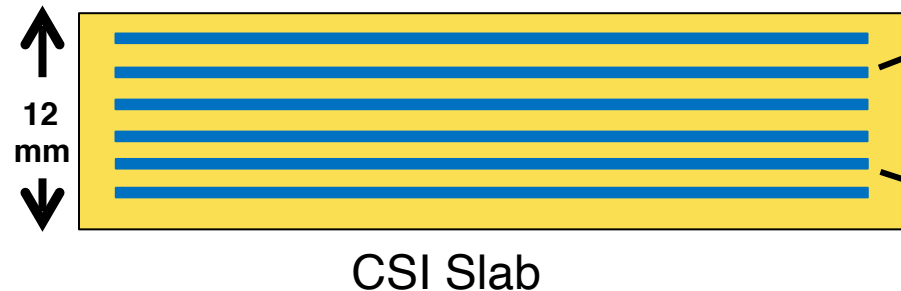
❑ Quantification metrics :

- ❖ Spectral quality
 - FWHM
- ❖ Extracted from scanner
- ❖ Shim quality
 - Field maps, before and after
 - $\sigma_{B_0}^{GLOBAL}$
 - Standard deviation of field map, over whole VOI
 - $\sigma_{B_0}^{LOCAL}$
 - Standard deviation of field map within each CSI voxel

Results – Field Maps

GRE parameters

- Resolution : 2.4mm in plane, 2mm slice
- Duration : 2 minutes
- 3T

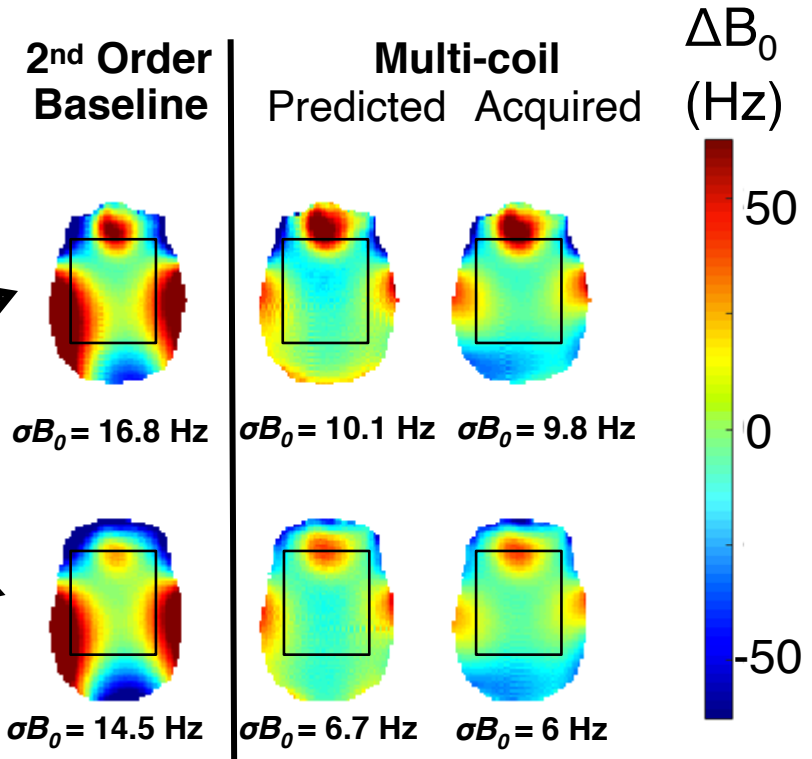


Prescribed Shim:

- ~14A of total current

LOCAL shim

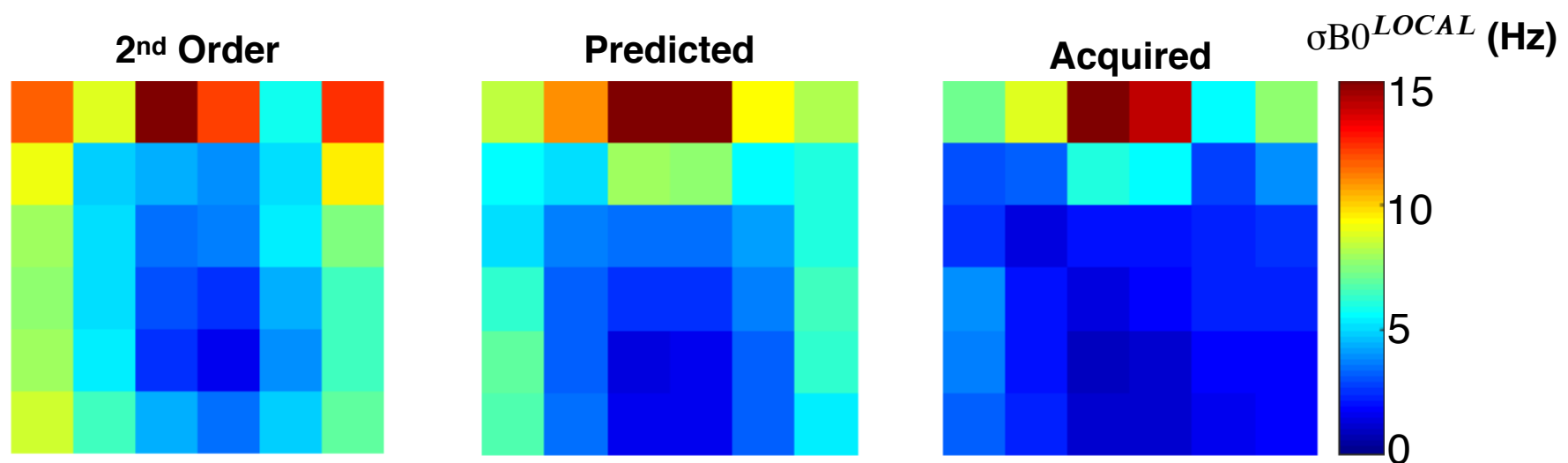
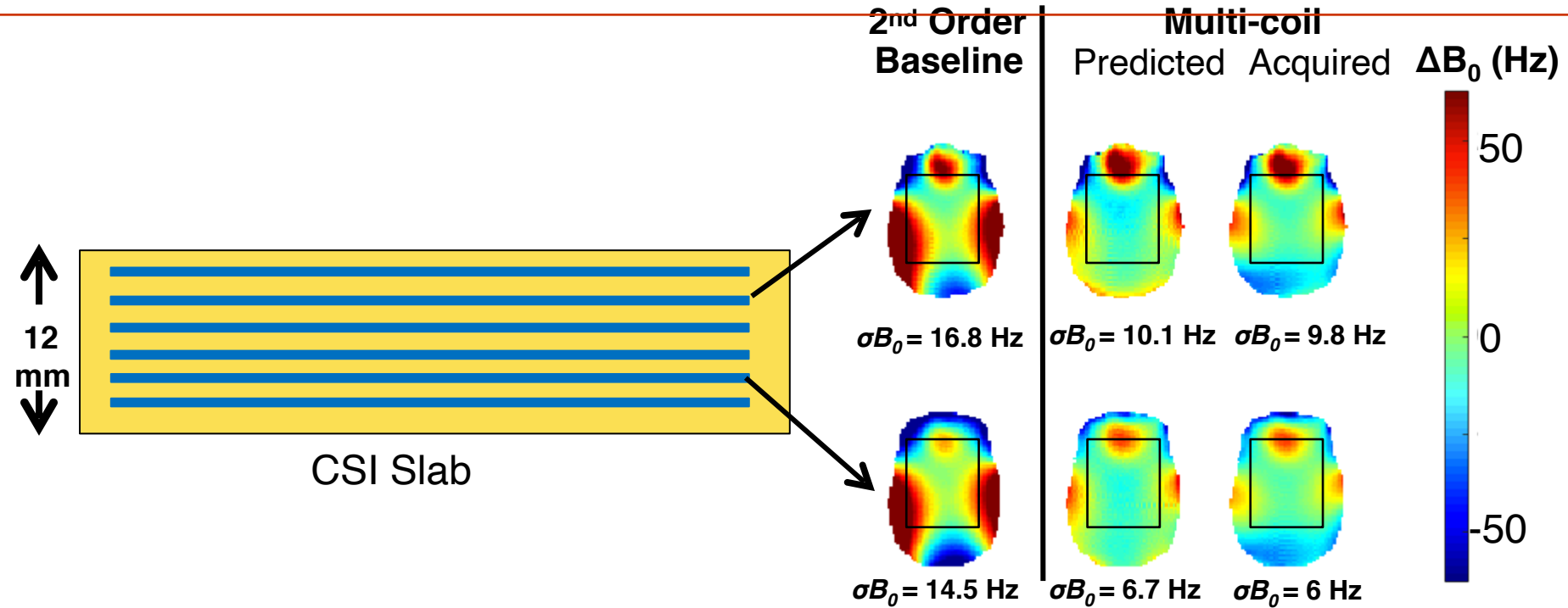
- ❖ Adjacent slices
- ❖ Separated by 2mm
- ❖ Overall thickness : 12mm



$\sigma B_0^{OVERALL SLAB}$

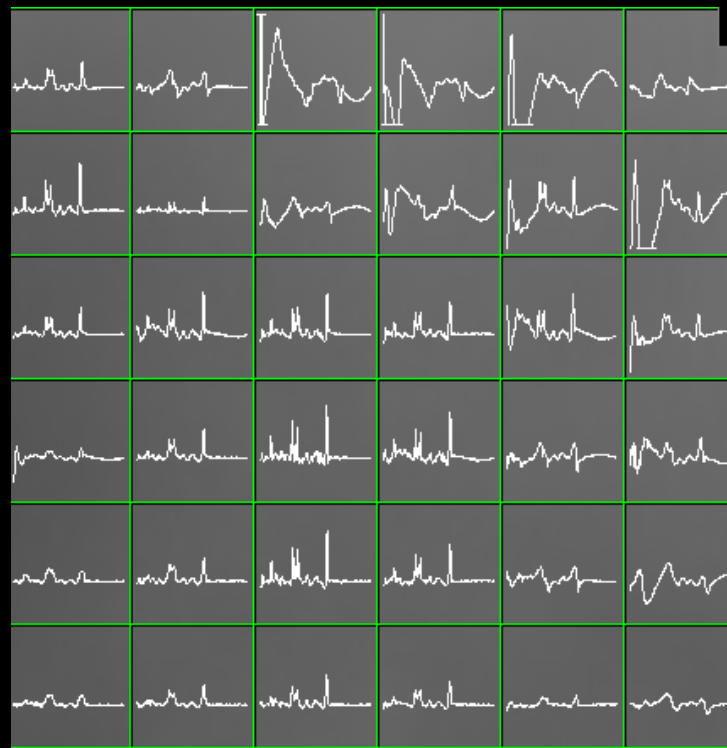
| 2 nd Order Baseline | Multi-coil |
|--------------------------------|------------|
| Predicted | Acquired |
| 15.8 Hz | 8.8 Hz |
| | 8 Hz |

Results – Field Maps – σB_0^{GLOBAL} and σB_0^{LOCAL}

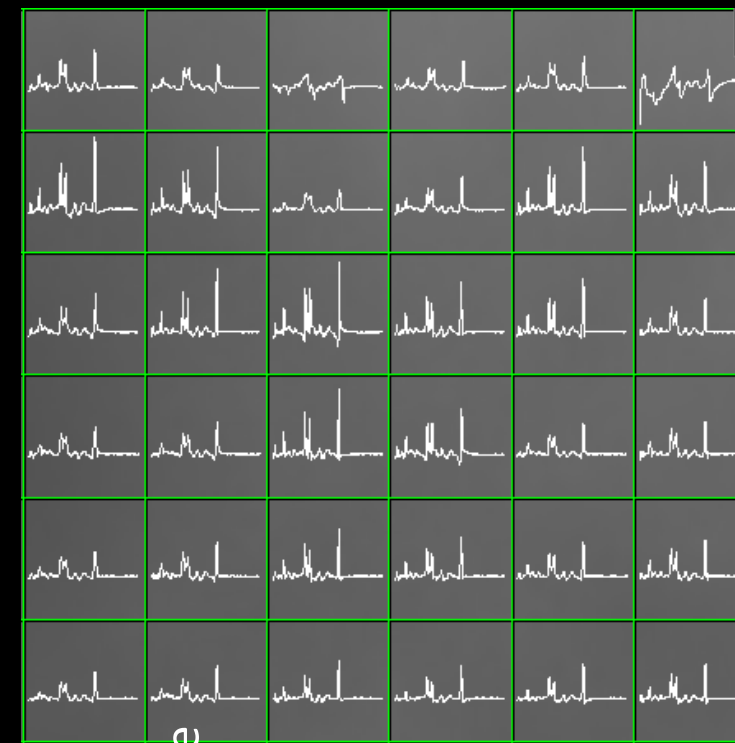


Results – Cartesian CSI – Phased Spectra

2nd Order



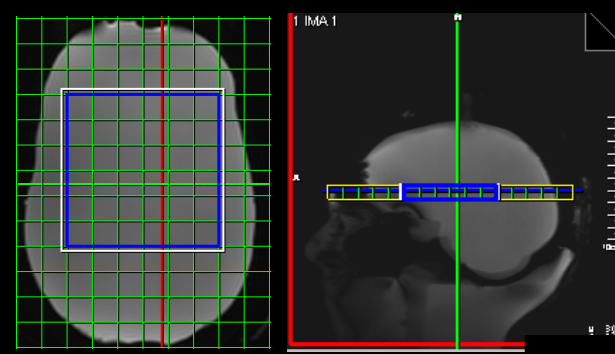
Shim Array



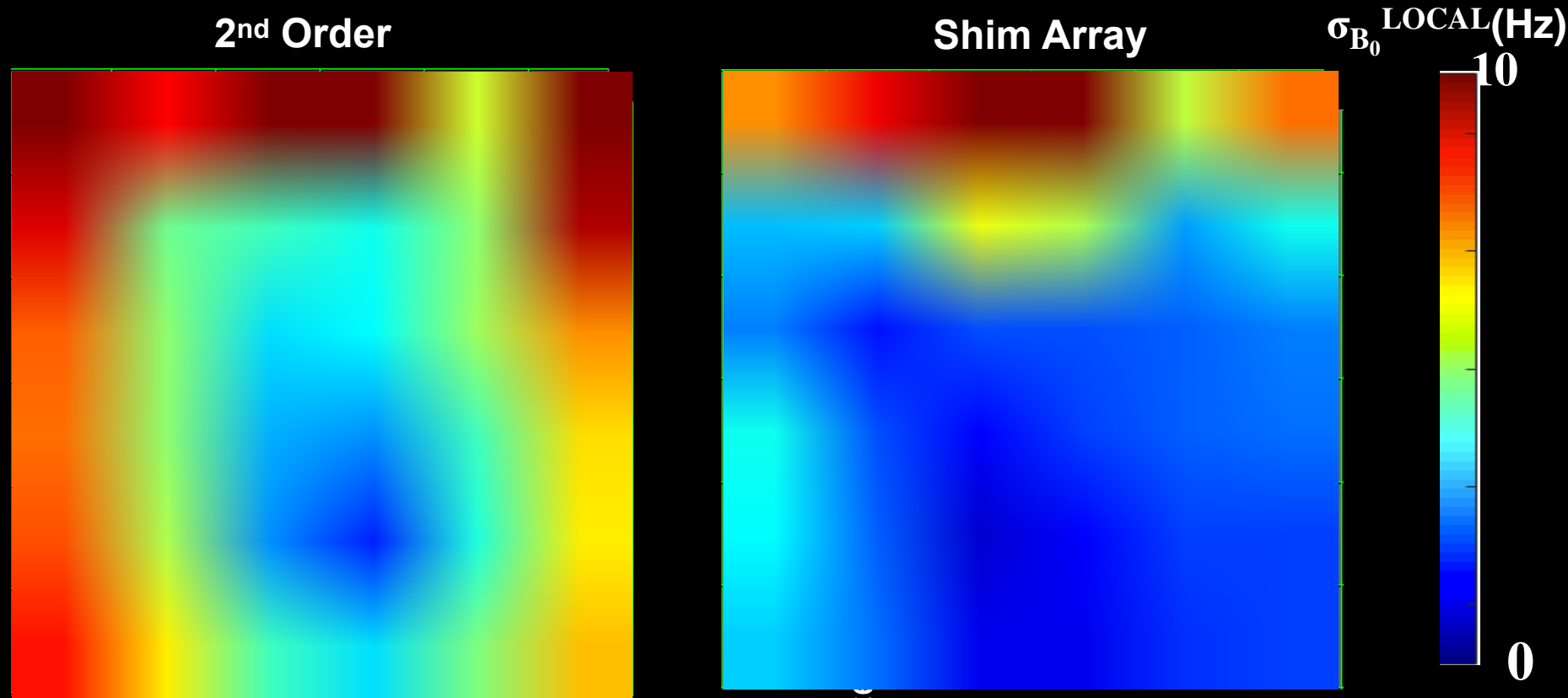
□ Parameters :

- ❖ TR/TE: 1400ms/144ms
- ❖ TA : 03:30
- ❖ Voxel Size : 2cc
- ❖ 2D

Geometric reference

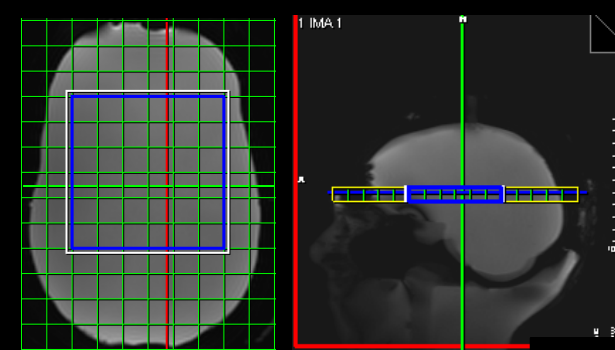


Results – Cartesian CSI – Phased Spectra



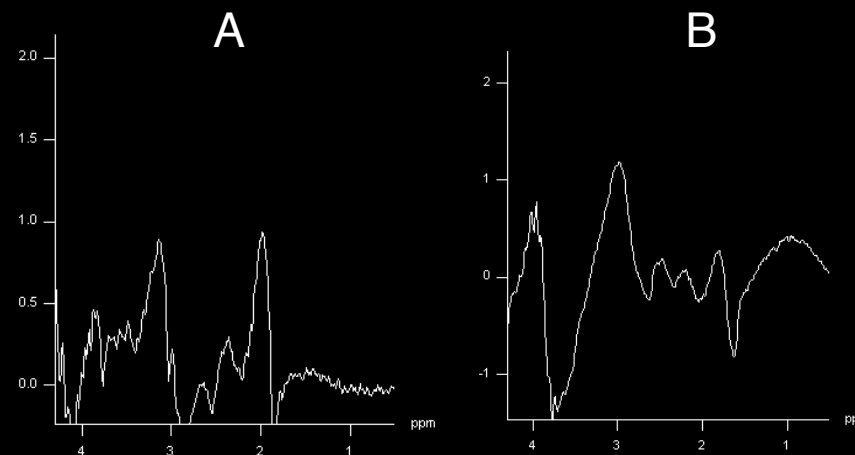
- Parameters :
- ❖ TR/TE: 1400ms/144ms
 - ❖ TA : 03:30
 - ❖ Voxel Size : 2cc
 - ❖ 2D

Geometric reference

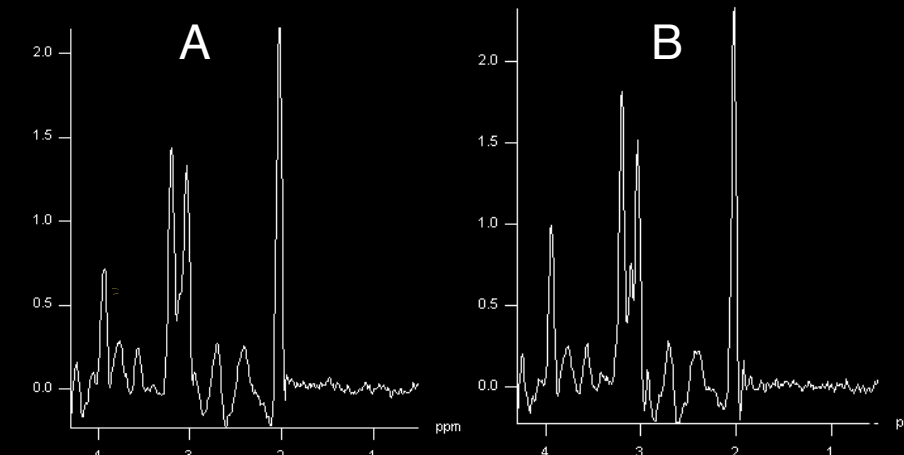


Results – Cartesian CSI – Phased Spectra

2nd Order

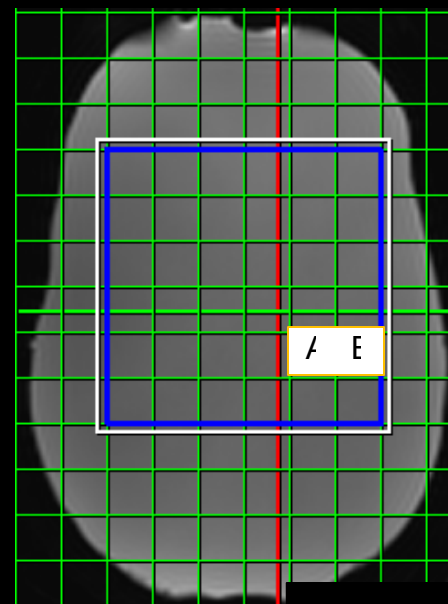


Shim Array



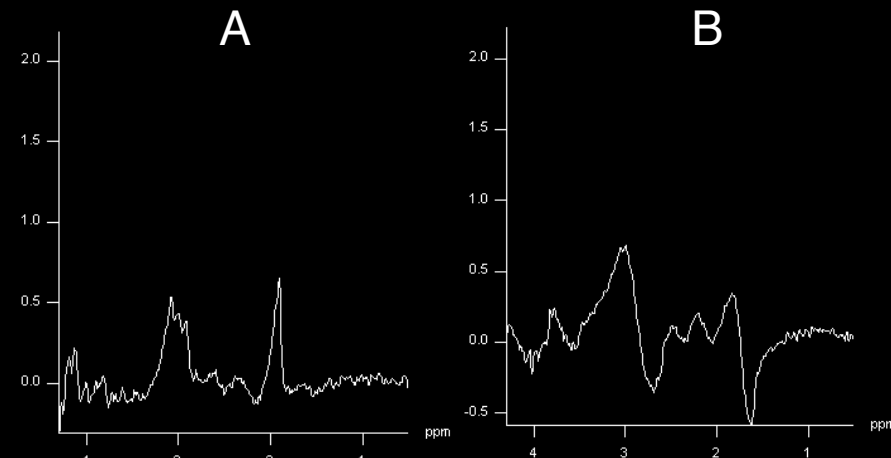
- Parameters :
 - ◆ TR/TE: 1400ms/144ms
 - ◆ TA : 03:30
 - ◆ Voxel Size : 2cc
 - ◆ 2D

Geometric reference

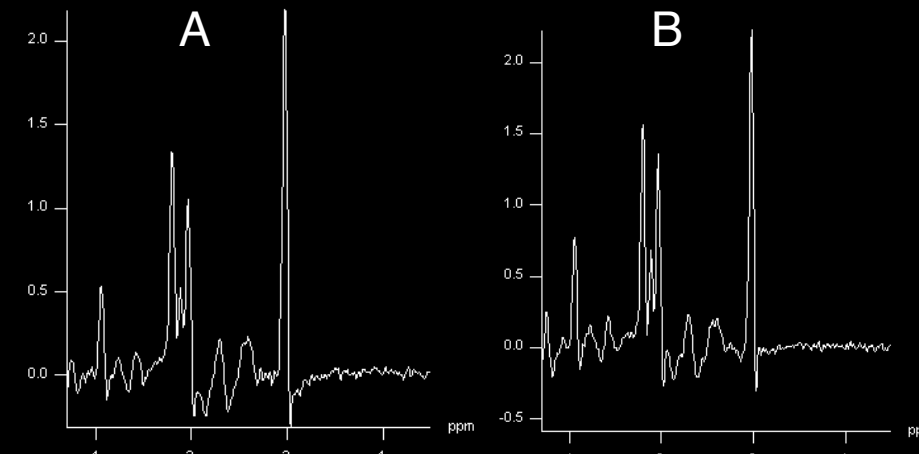


Results – Cartesian CSI – Phased Spectra

2nd Order

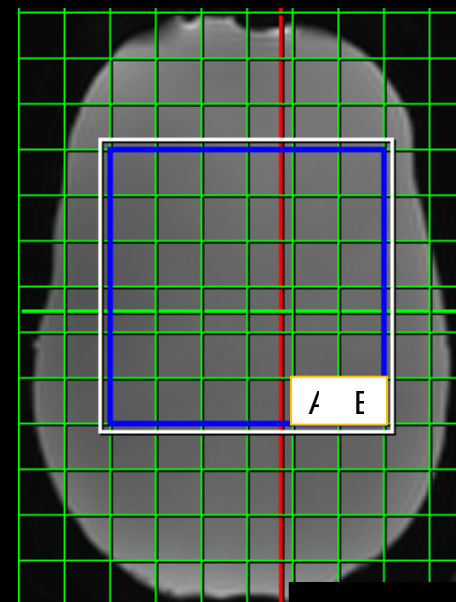


Shim Array



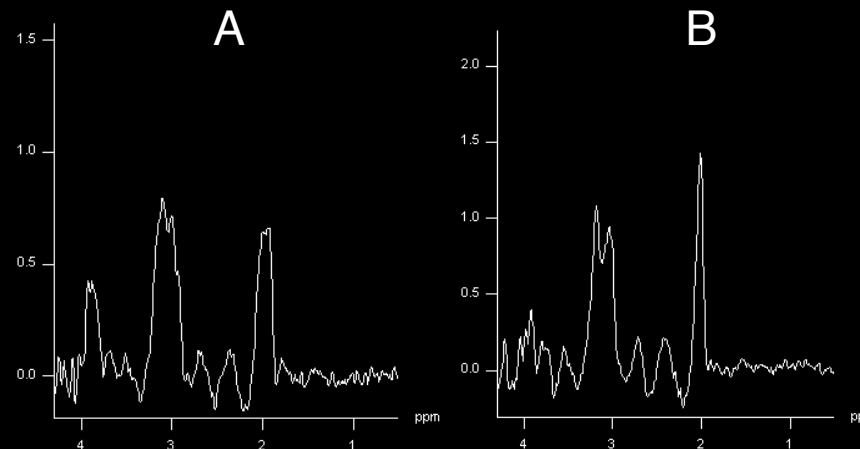
- Parameters :
 - ◆ TR/TE: 1400ms/144ms
 - ◆ TA : 03:30
 - ◆ Voxel Size : 2cc
 - ◆ 2D

Geometric reference

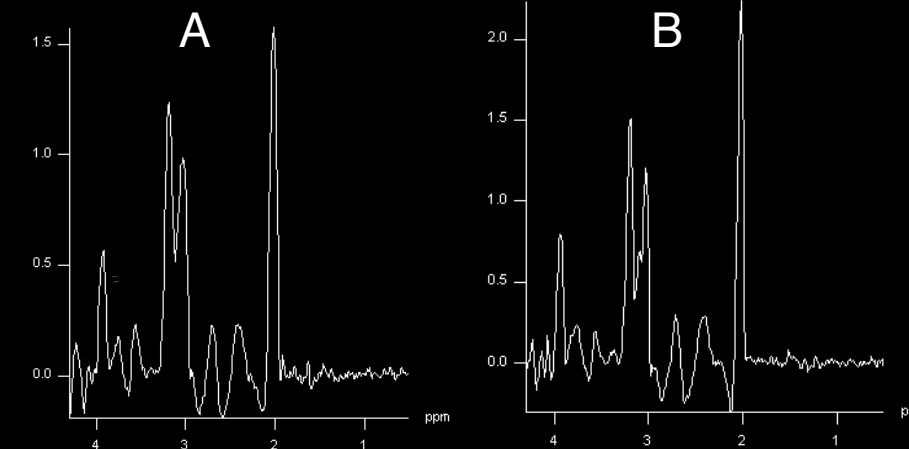


Results – Cartesian CSI – Phased Spectra

2nd Order

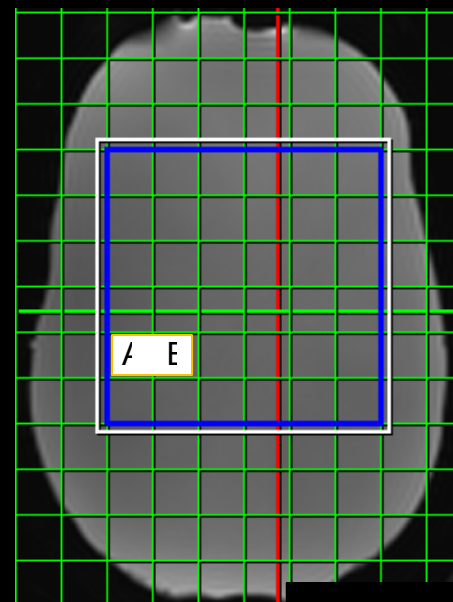


Shim Array



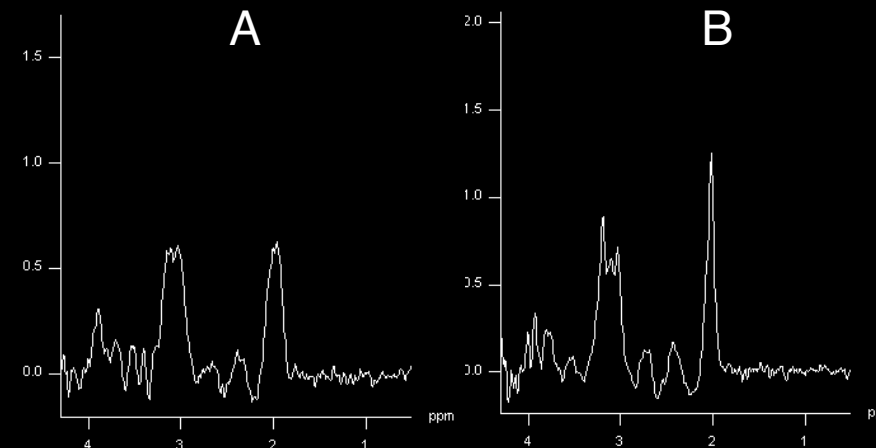
- Parameters :
 - ◆ TR/TE: 1400ms/144ms
 - ◆ TA : 03:30
 - ◆ Voxel Size : 2cc
 - ◆ 2D

Geometric reference

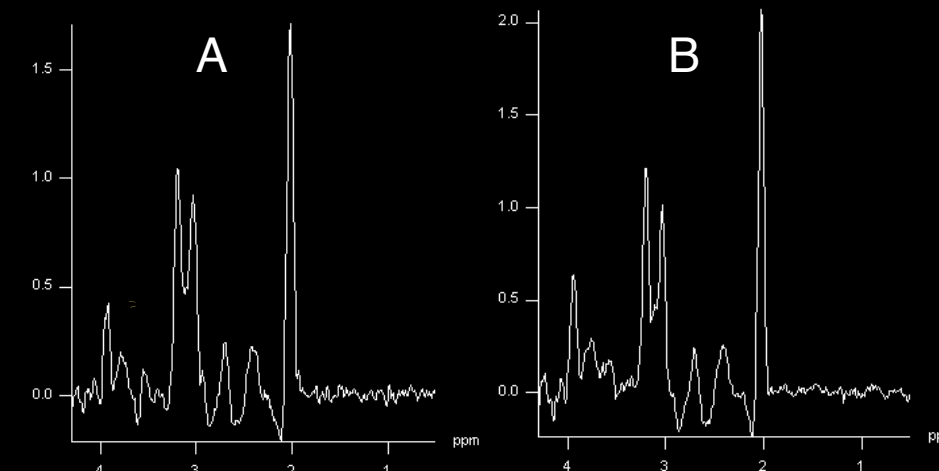


Results – Cartesian CSI – Phased Spectra

2nd Order

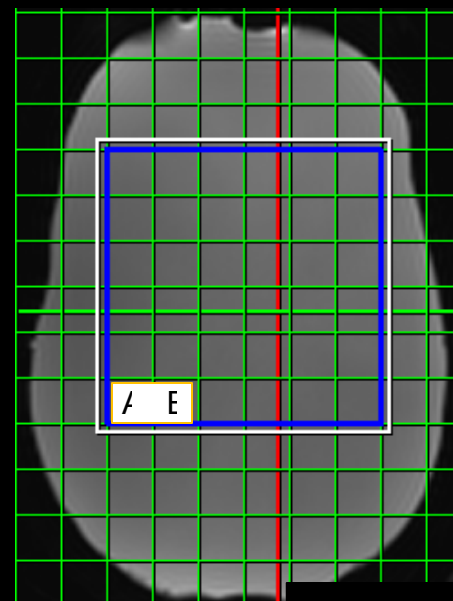


Shim Array



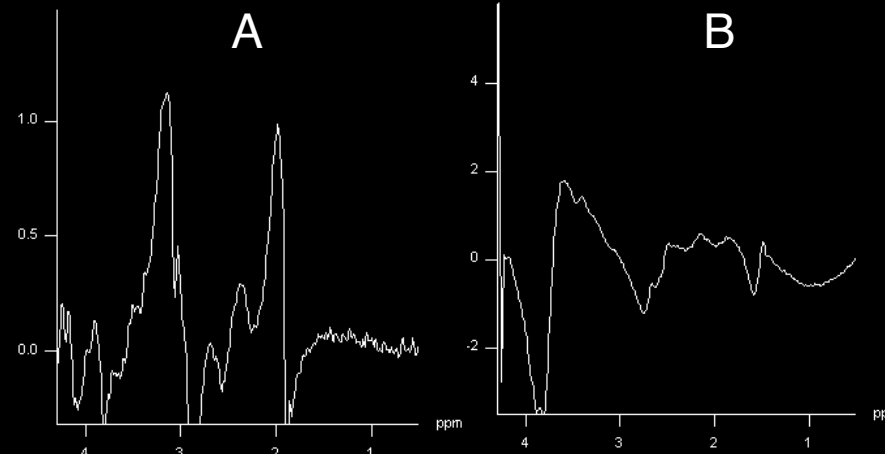
- Parameters :
 - ◆ TR/TE: 1400ms/144ms
 - ◆ TA : 03:30
 - ◆ Voxel Size : 2cc
 - ◆ 2D

Geometric reference

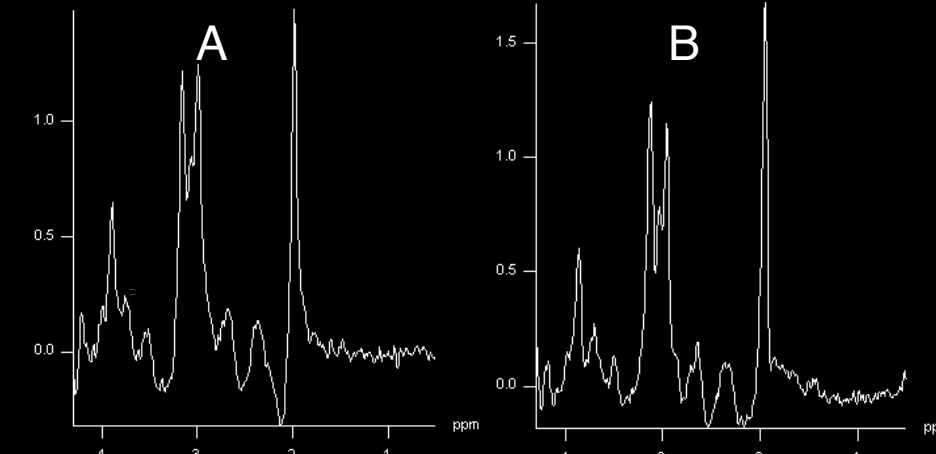


Results – Cartesian CSI – Phased Spectra

2nd Order

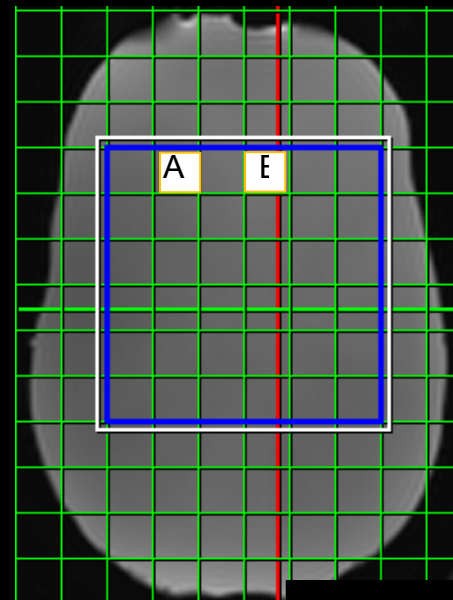


Shim Array



- Parameters :
 - ◆ TR/TE: 1400ms/144ms
 - ◆ TA : 03:30
 - ◆ Voxel Size : 2cc
 - ◆ 2D

Geometric reference



Results

- Improved spectral quality as judged by linewidths via MC shimming
 - ❖ 27% average linewidth narrowing
- Better water saturation via MC shimming
- Reduction in σB_0^{GLOBAL} as seen in field maps
 - ❖ 50% in overall CSI slab
 - ❖ Similar improvements per CSI slice
- Good agreement between predicted and acquired field maps

Acknowledgements and Related Talks

- ❑ We thank Trina Kok () for help preparing brain metabolite solution
- ❑ Jon Polimeni () for sharing his image acquisition and analysis scripts.
- ❑ This work is supported under
 - NIH R21 EB017338
 - P41 EB015896
 - BRP NIH R01EB017337



Related Talks:

- ❑ #1010 – R. Umesh – Multi-Dimensional Reduced Field-Of-View Excitation by Integrated RF Pulse and DYNAMITE B0 Field Design
- ❑ #1151 – W. Mattar – Multi-Coil B0 Shimming of the Human Heart: A Theoretical Assessment
- ❑ #1152 – I. Zivkovic – B0 Shimming at 9.4T Using a Multicoil Approach – Coil Design with Genetic Algorithm
- ❑ #1153 – J. Stockmann – Improving the Efficiency of Integrated RF-Shim Arrays Using Hybrid Coil Designs and Channel Placement and Compression Via a Genetic Algorithm
- ❑ #1154 – G. Germain – Optimization of Geometry for Combined RF/shim Coil Arrays for the Spinal Cord
- ❑ #1157 – N. Arango – Open-Source, Low-Cost, Flexible, Current Feedback-Controlled Driver Circuit for Local B0 Shim Coils and Other Applications
- ❑ #2198 – M. Jayatilake – STEREO-MC for Connected Spatiotemporal Excitation